DOI: 10.1002/chem.200702006

New Rare Earth Metal Complexes with Nitrogen-Rich Ligands: 5,5′-Bitetrazolate and 1,3-Bis(tetrazol-5-yl)triazenate—On the Borderline between Coordination and the Formation of Salt-Like Compounds

Patrick J. Eulgem,[a] Axel Klein,*[a] Nicola Maggiarosa,*[a, b] Dieter Naumann,[a] and Roland W. H. Pohl[a]

Abstract: From the two nitrogen-rich ligands BT^{2-} (BT = 5,5′-bitetrazole) and BTT^{3-} (BTT = 1,3-bis(1*H*-tetrazol-5-yl)triazene), a series of novel rare earth metal complexes were synthesised. For the BT ligand, a vast number of these complexes could be structurally characterised by single-crystal XRD, revealing structures ranging from discrete molecular aggregates to salt-like compounds. The isomorphous complexes $[La_2(BT)_3]\cdot 14H_2O$ (**1**) and $[Ce_2(BT)_3]\cdot 14H_2O$ (**2**) reveal discrete molecules in which one BT^{2-} acts as a bridging ligand and two BT groups as chelating ligands. The complexes, $[M(BT)(H_2O)_7]_2[BT]\cdot xH_2O$ (**3**–**5**), (M = Nd (**3**), Sm (**4**), and Eu (**5**)), are also isomorphous and consist of $[M(BT)(H_2O)_7]^+$ ions in which only one BT^{2-} acts as a chelate ligand for each metal centre. $[Tb(H_2O)_8]_2[BT]_3\cdot xH_2O$ (**6**) and $[Er(H_2O)_8]_2[BT]_3\cdot xH_2O$ (**7**) are salt-like compounds that do not exhibit any significant metal–nitrogen contacts. In the BTT–samarium compound **9**, discrete molecules were found in which BTT^{3-} acts as a tridentate ligand with three Sm−N bonds.

Keywords: coordination modes · IR spectroscopy · lanthanides · N ligands · X-ray diffraction

Introduction

Nitrogen-rich, N-heterocyclic ligands, such as triazoles and tetrazoles, have various points of interest. The ligand molecules themselves can be perceived as high-energy materials[1–4] or nitrogen-generating agents.[1,5] They have also recently become of enormous interest in view of their ready preparation by means of so called “click” chemistry.[6] From the viewpoint of coordination chemistry, they represent a very interesting class of ligands that are mainly characterised by their extremely low-lying π*-orbitals, which makes them excellent π-acceptors.[7] Such strong π-acceptor ligands were frequently used, for example, for the construction of complexes with interesting optical or electrochemical properties, with applications in non-linear optic (NLO) materials,[8] electronic devices (switches or wires)[9] or multielectron catalysis.[7c,10] In transition-metal complexes, they are usually combined with electron-rich (low oxidation state), late transition metals of the d-block, such as Cu^{II}, Re^{I} or Ru^{II}, allowing for rather stable as well as moisture and oxygen insensitive materials. For applications in materials science, the construction of binuclear complexes (or complexes of even higher nuclearity) is often desirable.

The chemistry of early transition metals or lanthanides with nitrogen-rich, N-heterocyclic ligands is much less developed, which is a pity in view of the interesting properties that can be expected for such compounds, such as intense luminescence or strong Lewis acidity.

The 5,5′-bitetrazole (H_2BT)[11–13] molecule and its dianion BT^{2-} are interesting candidates for rich coordination

[a] Dr. P. J. Eulgem, Prof. Dr. A. Klein, Dr. N. Maggiarosa, Prof. Dr. D. Naumann, R. W. H. Pohl
Universität zu Köln
Institut für Anorganische Chemie
Greinstrasse 6, 50939 Köln (Germany)
Fax: (+49) 221-4704899
E-mail: axel.klein@uni-koeln.de
maggnico@lgchem.com

[b] Dr. N. Maggiarosa
Present address: LG Chem., Ltd.
Research Park, Chemicals and Polymers R&D
104-1 Moonji-dong, Yuseong-gu
Daejeon, 305-380 (Korea)

Supporting information for this article is available on the WWW under http://www.chemeurj.org/ or from the author and contains figures showing the crystal structure (unit cell) of $[Sm(BTT)]\cdot 8H_2O$ (**9**), IR spectra of Na_2BT, $[Ce_2(BT)_3]\cdot xH_2O$ and $[Tb_2(BT)_3]\cdot xH_2O$, a luminescence spectrum of bulk $[Tb_2(BT)_3]\cdot xH_2O$, a photograph of $[Tb_2(BT)_3]\cdot xH_2O$ and a powder XRD pattern of **9**.

chemistry. They contain eight nitrogen atoms and may act as mono-, bi-, tri- or tetradentate ligands. Scheme 1 depicts various binding modes for the dianion BT^{2-}. Bitetrazolate should thus allow the preparation of mononuclear, binuclear or oligonuclear complexes (coordination polymers), as well as the formation of one-, two- or three-dimensional networks in solid structures.

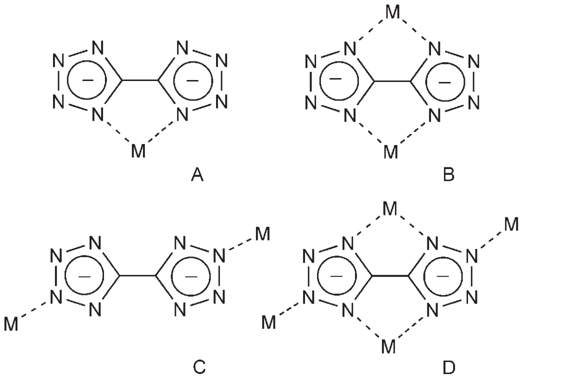

Scheme 1. Feasible coordination modes of BT^{2-}. **A**: chelate η^2; **B**: chelate bridging $\mu,\eta^2:\eta^2$; **C**: monodentate bridging $\mu,\eta^1:\eta^1$ and **D**: mono- and bidentate bridging.

It is, therefore, surprising that there are only a few reports on transition-metal complexes of 5,5′-bitetrazole (BT) or its dianion (BT^{2-}). Syntheses and ^1H NMR spectra for the complexes $[Ru(BT)(N\frown N)_2]$ ($N\frown N$ = 2,2′-bipyridine or 4,4′-dimethyl-2,2′-bipyridine) have been reported, but these compounds were never isolated or fully characterised.[14] The same is also true for a chloro-bridged dinuclear Pd^{II} complex.[14] In contrast, there are numerous reports on the use of metal-containing salts of 5,5′-bitetrazole as highly energetic materials[5,15,16] or N_2 sources, including a number of patents.[17]

Starting from 5,5′-bitetrazolate BT^{2-}, the consecutive introduction of additional NH groups leads to a series of tetrazolyl bridging ligands $[N_4C-(NH)_n-CN_4]^{2-}$ (see Scheme 2).[12]

The first member ($n=1$) of the series is the dianion of *N,N′*-bis(1(2)*H*-tetrazol-5-yl)amine (H_2BTA). It was recently successfully used to prepare Cu^{II} complexes $[Cu(BTA)(NH_3)_2]\cdot x\,H_2O$ ($x=0$, 1 or 2.5) that show extended networks in the solid state with the N3 atom bridging to the copper atom of the next molecular entity, which results in a square pyramidal geometry around the copper atom.[18]

From the next member of the series, which is the dianion of *N,N′*-bis(1(2)*H*-tetrazol-5-yl)hydrazine (H_2BTH), the barium compound $[Ba(BTH)(N_2H_4)_3]$ was structurally characterised and found to exhibit a typical structural pattern for a salt-like compound. Three BTA dianions and six hydrazine molecules bind to the barium atoms in a tricapped trigonal prism.[19] From the dehydrogenated derivative 5,5′-azotetrazolate (AT^{2-}), a large number of salt-like compounds $[M_r(AT)_s(H_2O)_x]$ containing alkaline metals ($r=2$, $s=1$), earth alkaline metals ($r=s=1$), Al and the rare earth elements Y, La, Ce, Nd and Gd ($r=2$, $s=3$) are known.[1b,5] They were thoroughly characterised by NMR and IR spectroscopy and, in part, by crystal structure determination. None of these compounds exhibits the coordination pattern around the metal atom that one would expect for a metal complex; therefore, they can all be considered as salt-like compounds.

The next member ($n=3$) of the series in Scheme 2 is the trianion BTT^{3-} of 1,3-bis(1*H*-tetrazol-5-yl)triazene (H_3BTT), which, in very early work, was described as a potent explosive in combination with heavy metals such as Pb^{II}.[20] A close derivative of BTT^{3-} BMTT (BMTT = 1,3-bis(2-methyltetrazol-5-yl)triazenide) is known to form a neutral nickel complex $[Ni(BMTT)_2]$ in which two deprotonated azenide groups compensate for the 2+ charge of the nickel atom and the tetrazole ligands are neutral.[21]

Taking into account these studies, we considered 5,5′-bitetrazole (H_2BT) and 1,3-bis(1*H*-tetrazol-5-yl)triazene (H_3BTT) or rather their anionic forms BT^{2-} and BTT^{3-}, respectively, as suitable bridging ligands for the preparation of new mono- and binuclear complexes of a number of rare-earth elements. The first results of this study will be presented in this paper.

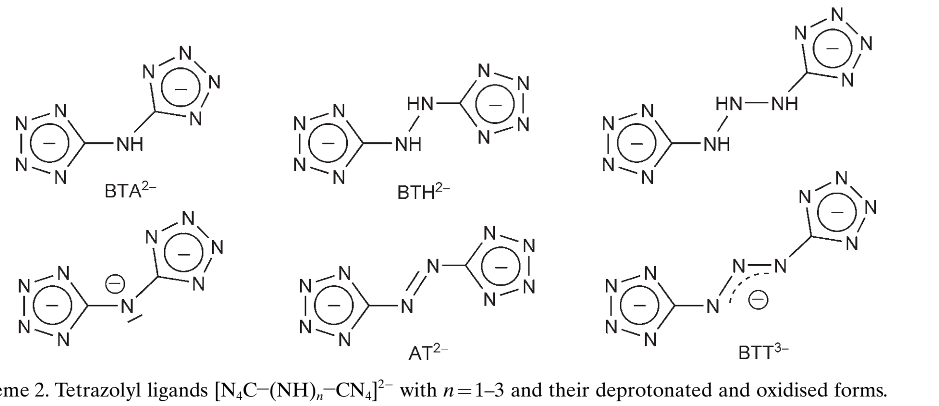

Scheme 2. Tetrazolyl ligands $[N_4C-(NH)_n-CN_4]^{2-}$ with $n=1$–3 and their deprotonated and oxidised forms.

Results and Discussion

Synthesis of the starting materials H_2BT, MnBT, Na_2BT and BaBT: The first reference dealing with the preparation of 5,5′-bitetrazole H_2BT dates back to 1914.[11a,b] The reaction of a concentrated aqueous solution of HN_3 with cyanogen was described [Eq. (1)].

In a comparatively convenient and less-dangerous manner 5,5′-bitetrazolate can be prepared in the form of its manga-

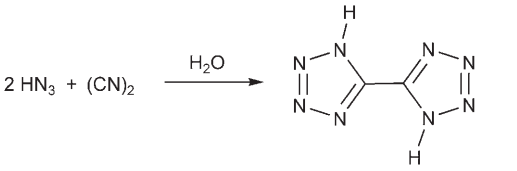

(1)

nese salt MnBT by the copper-catalysed reaction of MnO_2, NaCN and NaN_3 reported by W. Friedrich in 1956 [Eq. (2)].[11c]

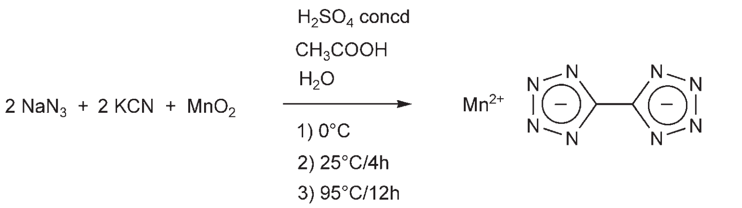

(2)

We found that MnBT is an ideally suited precursor for the synthesis of Na_2BT, H_2BT and BaBT [Eq. (3)] (for details see the Experimental Section).

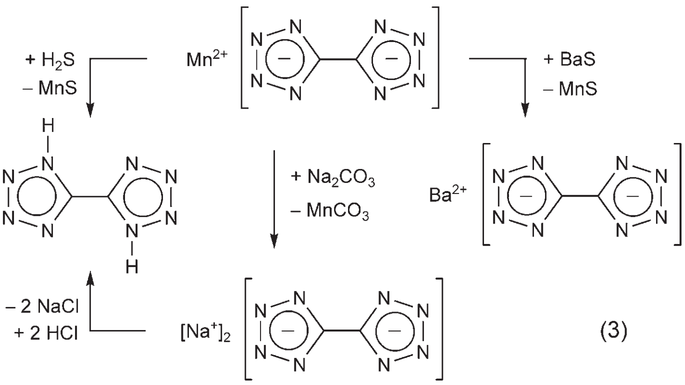

(3)

BaBT was used for the preparation of the rare earth metal compounds, making use of the sparingly soluble nature of $BaSO_4$ in aqueous medium (see below). The rare earth metal sulphates are all commercially available.

The sodium salt of 1,3-bis(1*H*-tetrazol-5-yl)triazene, Na_3BTT, can be obtained by reacting $(HN)(H_2N)CNH$-$(NH_2){\cdot}HNO_3$ with $NaNO_2$ in aqueous solution according to Thiele or Hofmann's procedure [Eq. (4)].[22]

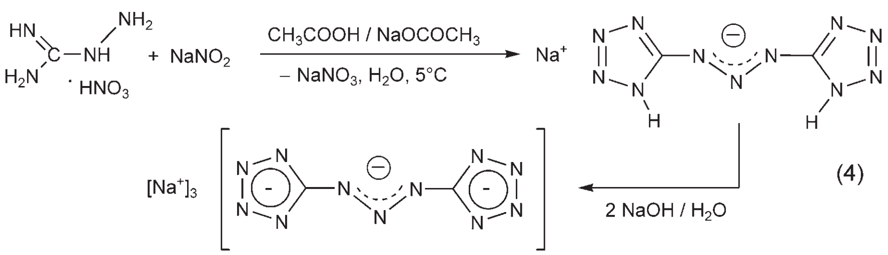

(4)

NMR spectroscopy of BaBT, Na_2BT and Na_3BTT: For the first time, the two ligands BT^{2-} and BTT^{3-} in their deprotonated form could be characterised by using NMR spectroscopy. The carbon atoms of both the barium and the sodium salt of 5,5′-bitetrazole exhibit signals in the ^{13}C NMR spectrum at $\delta = 154.3$ ppm, indicating complete dissociation in aqueous solution. The ^{14}N NMR spectrum shows two signals at $\delta = 16$ and -52 ppm, which are largely broadened due to the quadrupole moment of ^{14}N ($I = 1$). A ^{15}N NMR spectrum could not be recorded owing to the poor solubility of both BT compounds.

The carbon shifts of the 1,3-bis(tetrazol-5-yl)triazene anion (BTT^{3-}; Na salt) are found in the ^{13}C NMR spectrum at $\delta = 171.4$ ppm. In Figure 1, the ^{15}N NMR spectrum of $Na_3[(N_4C)N_3(CN_4)]$ with signals at $\delta = 108.5$, -6.9, -93.7 and -95.1 ppm is depicted. The corresponding ^{14}N NMR spectrum reveals the same signals; however, they are dramatically broadened. Comparable values have been reported for the sodium salt of 5,5′-azotetrazolate (AT).[5]

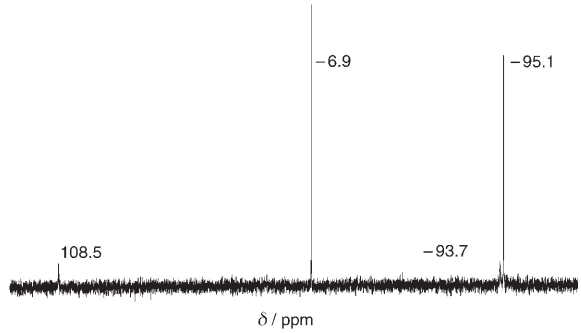

Figure 1. ^{15}N NMR spectrum for $Na_3[(N_4C)N_3(CN_4)]$ in D_2O.

Preparation of the BT^{2-} complexes: BaBT was used as a starting material and all title compounds were obtained from reactions with the respective metal sulfates [Eq. (5)].

In the reactions with $La_2(SO_4)_3$ and $Ce_2(SO_4)_3$, colourless crystals of the composition $[La_2(BT)_3]{\cdot}14H_2O$ (**1**) and $[Ce_2(BT)_3]{\cdot}14H_2O$ (**2**) were obtained after barium sulphate had been filtered off and water had been evaporated (for the crystal structures of **1** see Figure 3). Elemental analyses of bulk (microcrystalline) material of **1** and **2** correspond roughly to calculated values for $[M_2(BT)_3]{\cdot}20H_2O$. In fact, assuming the correct C and N values (the C/N ratio is always correct!), the number of water molecules lies at 21 for Ce and

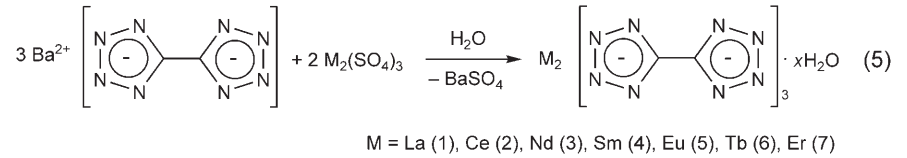

22.5 for La (for details, see the Experimental Section). Upon heating in vacuo, compounds **1** and **2** loose water up to a decomposition temperature of about 350 °C. At this temperature, violent explosions occurred.

The corresponding reaction of $Ce(SO_4)_2$ with BaBT proceeded smoothly yielding a precipitate which showed the characteristic yellow colour of Ce^{IV} compounds. An evolution of gas, as reported by Klapötke et al. for the reaction of $Ce(SO_4)_2$ with BaAT[5] (AT = 5,5′-azotetrazolate) was not observed. Elemental analysis of the material points to a mixture of $[Ce(BT)_2]$ and $BaSO_4$; however, as a result of the complete insolubility of the material, we were not able to purify the product $[Ce(BT)_2]$, nor did we obtain single crystals from the mixture.

All other 5,5′-bitetrazolate compounds (**3**–**7**) were obtained in a similar manner by slow evaporation of water, either by cautious heating or simply by storing solutions for a longer period at ambient atmosphere in open glass beakers. Upon dehydratation of some of the compounds, decomposition to colourless substances (identified as the corresponding rare earth metal oxides and H_2BT) was observed. Thus, hydrolysis reactions might be a serious reason for the low yields obtained for these compounds. The ease of hydrolysis surely depends on the acidity of the metal–water complexes of the trivalent rare earth metal ions, which increases along the series of lanthanides. The elemental analyses for compounds **3**–**7** agree quite well with the formulae $[M_2(BT)_3]\cdot 20\,H_2O$. The water contents obtained for the bulk material, assuming the correct C and N values, only range from 19 (Er) to 20.5 (Nd). A full table with elemental analyses and further analytical (MS) or spectroscopic data (IR) of these new compounds is collected in the Experimental Section.

Unfortunately, the compounds are extremely insoluble in water or organic solvents, preventing their spectroscopic characterisation by NMR or IR spectroscopy in solution and even the recording of negative ESIMS spectra. At a first glance, the colours of the compounds closely resemble those of the corresponding rare earth metal sulphates. This is not unexpected, as these absorption bands are of pure ligand field (f–f) character and thus, largely independent of the ligand field (or surrounding).[23] Nevertheless, a thorough investigation of their absorption and emission properties is underway. As we obtained single crystals for compounds **1** to **7**, this report will discuss in detail the crystal and molecular structures of the compounds (see below).

Preparation of the BTT^{3-} complexes: Complexes with the BTT^{3-} ligand were synthesised by mixing the sodium salt of 1,3-bis(1*H*-tetrazol-5-yl)triazene (H_3BTT), Na_3BTT and the corresponding rare earth metal chlorides MCl_3 in water at 25 °C [M = Nd (**8**), Sm (**9**), Eu (**10**), Er (**11**)]. Characteristically coloured amorphous materials were obtained that analysed according to the formula $[M(BTT)]\cdot 10\,H_2O$ (see the Experimental Section). Unfortunately, the solubility of the compounds is extremely poor (in DMF or DMSO they decompose without dissolving) and the tendency to explode in the solid state is even enhanced relative to the compounds with the BT^{2-}. Therefore, analytical or spectroscopic characterisation of the compounds **8**, **10** and **11** has been restricted so far to elemental analyses. However, as in the case of M = Sm **9**, we obtained single crystals for a crystal structure determination and we also recorded an IR spectrum, calculated the corresponding IR frequencies (DFT) and submitted the bulk material to a powder X-ray diffraction experiment (see below).

Thermal properties of the rare earth metal–BT compounds: The 5,5′-bitetrazolate of Eu^{III} (**5**) (as a model compound for the entire series) is expected to decompose explosively upon rapid heating, in a similar manner to other compounds with high-nitrogen content. Our experiments to determine the melting point showed that the hydrated complex **5** decomposes explosively at 350 °C. As a consequence, thermal stability was studied only within the temperature range of 30 to 300 °C.

As shown in Figure 2, the compound is dehydrated within the temperature range of 30–180 °C and very probably converted into the anhydrous complex $[Eu_2(BT)_3]$. The loss of water ligands is expressed by three weakly endothermal peaks and a comparably strong endothermal effect at approximately 180 °C. We assume that the reaction starts from the (nine-coordinated) binuclear species $[(BT)(H_2O)_6Eu(\mu\text{-}BT)Eu(BT)(H_2O)_6]$. Above 190 °C, the onset of a moderate decomposition of the anhydrous complex is monitored,

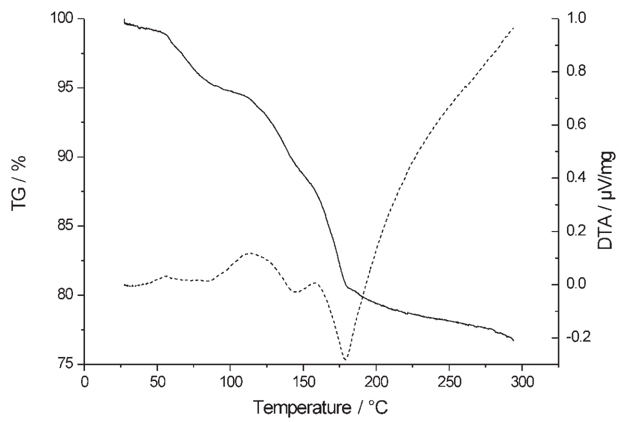

Figure 2. DTA/TG for $[Eu(BT)(H_2O)_7]_2[BT]\cdot xH_2O$; TG = ——, DTA = -----.

which probably gives rare earth metal nitride or rare earth metal carbide–nitride compounds.

Crystal and molecular structures of the BT compounds: Although the crystal structures of the compounds **1–7** were all found to be part of the space group $P\bar{1}$ (see crystallographic data in Table 1), they exhibit three different structural types.

The first structural type is represented by the structures of the complexes $[La_2(BT)_3]\cdot 14H_2O$ (**1**) and $[Ce_2(BT)_3]\cdot 14H_2O$ (**2**) in which one BT acts as a bridge between two rare earth metal atoms and a second BT acts as a chelate ligand for each rare-earth metal, building a N–M–N′ core. The bridging BT is linked through the nitrogen atoms at the 2- and 2′-positions, and the chelating BT through the nitrogen atoms at the 1- and 1′-positions (Figure 3). Two molecules of H_2O are intercalated in the crystal structure.

The second structural type is found for the molecular structures of the complexes **3** to **5** $[M(BT)(H_2O)_7]_2[BT]\cdot xH_2O$, M = Nd, Sm, and Eu, and consists of $[M(BT)(H_2O)_7]^+$ units with BT^{2-} coordinated in a chelate fashion to the rare-earth metal through the nitrogen atom at the 1- and 1′-positions, and also through well separated BT^{2-}. For examples, see Figures 4 and 5.

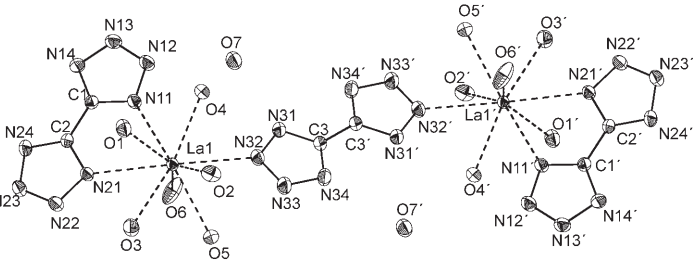

Figure 3. Motif of **1** (thermal ellipsoids represent 50% probability), hydrogen atoms are omitted for clarity. Selected bond lengths [Å]: La1−O1 2.546(10), La1−O2 2.484(15), La1−O3 2.623(17), La1−O4 2.502(15), La1−O5 2.546(9), La1−O6 2.516(13), La1−N11 2.726(17), La1−N21 2.769(10), La1−N32 2.741(11); symmetry operation for equivalent atoms: i: $1-x$, $-y$, $1-z$.

Finally, the third structural type is represented by $[Tb(H_2O)_8]_2[BT]_3\cdot xH_2O$ (**6**) and $[Er(H_2O)_8]_2[BT]_3\cdot xH_2O$ (**7**), which are salt-like compounds with well-separated BT^{2-} and $[M(H_2O)_x]^{3+}$ ions without any significant M–N contacts (Figure 6).

Bond lengths and angles of all tetrazole rings in the 5,5′-bitetrazolate compounds **1–7** (Table 2) are very close to each other and also correspond to values reported for struc-

Table 1. Summary of crystallographic data for **1–7** and **9**.

	1	**2**	**3**	**4**	**5**	**6**	**7**	**9**
empirical formula	$C_3H_{14}LaN_{12}O_7$	$C_3H_{14}CeN_{12}O_7$	$C_3H_{20}N_{12}NdO_{10}$	$C_3H_{20}N_{12}SmO_{10}$	$C_3H_{20}N_{12}EuO_{10}$	$C_3H_{20}N_{12}TbO_{10}$	$C_3H_{20}N_{12}ErO_{10}$	$C_2H_{16}N_{11}SmO_8$
F_w [g mol^{-1}]	469.7	470.38	528.55	534.5	536.27	543.23	551.57	472.62
colour, habit	colourless, prism	colourless, prism	blue, prism	yellow, prism	colourless, prism	colourless, plate	pink, needle	colourless–yellow, prism
T [K]	293 (2)	293 (2)	170 (2)	293 (2)	170 (2)	293 (2)	293 (2)	293 (2)
crystal size [mm]	0.2 × 0.15 × 0.1	0.18 × 0.2 × 0.15	0.15 × 0.3 × 0.2	0.1 × 0.15 × 0.2	0.2 × 0.2 × 0.25	0.06 × 0.2 × 0.15	0.1 × 0.1 × 0.2	0.1 × 0.1 × 0.1
crystal system	triclinic	triclinic	triclinic	triclinic	triclinic	triclinic	triclinic	monoclinic
space group	$P\bar{1}$	$P\bar{1}$	$P\bar{1}$	$P\bar{1}$	$P\bar{1}$	$P\bar{1}$	$P\bar{1}$	$C2/c$
a [Å]	7.519(1)	7.4985(14)	9.0948(12)	9.0753(15)	9.068(1)	8.3163(12)	8.2951(14)	7.2141(17)
b [Å]	7.5998(10)	7.5777(15)	9.2820(12)	9.3630(17)	9.233(1)	10.4566(15)	10.4235(17)	14.649(4)
c [Å]	13.5659(17)	13.522(3)	10.9285(14)	10.986(2)	10.891(1)	10.9904(18)	10.986(2)	13.419(4)
α [°]	84.38(1)	84.33(2)	99.160(1)	99.67(2)	99.15(1)	94.681(12)	94.82(2)	90
β [°]	78.58(1)	78.89(2)	93.56(1)	93.17(2)	93.68(1)	96.207(12)	96.27(2)	97.25(3)
γ [°]	74.94(1)	74.96(2)	112.397(9)	112.719(19)	112.45(1)	113.018(11)	113.019(18)	90
V [Å^3]	732.687(17)	747.7(3)	834.4(2)	841.4(3)	824.3(2)	866.4(2)	860.6(3)	1406.8(7)
Z	2	2	2	2	2	2	2	4
ρ_{calcd} [g cm^{-3}]	2.126	2.148	2.104	2.110	2.136	2.082	2.128	2.231
μ [mm^{-1}]	2.976	3.104	3.190	7.13	1.941	4.1730	9.90	4.24
F(000)	458	460	524	528	259	534	540	924
Θ range [°]	2.78 to 29.57	2.75 to 29.28	1.90 to 29.61	2.41 to 28.04	1.91 to 29.57	1.88 to 29.62	2.65 to 28.10	2.78 to 28.03
index range	$-10<h<10$ $-10<k<10$ $-18<l<18$	$-9<h<9$ $-9<k<9$ $-17<l<17$	$-12<h<12$ $-12<k<12$ $-15<l<15$	$-11<h<12$ $-12<k<12$ $-14<l<14$	$-12<h<12$ $-12<k<12$ $-15<l<15$	$-11<h<11$ $-12<k<14$ $-15<l<13$	$-10<h<10$ $-13<k<13$ $-14<l<14$	$-9<h<9$ $-19<k<19$ $-17<l<17$
reflns collected	14021	8602	16410	10141	14983	11183	10367	6500
independent reflns	4073	3199	4637	3752	4574	4779	3837	1695
observed reflns (2σ)	3905	3101	4322	3141	3971	3829	3010	1311
R_{int}	0.0661	0.0587	0.0306	0.0482	0.0239	0.0303	0.058	0.2834
data/restraints /parameters	4073/0/266	3199/0/266	4637/0/317	3752/41/317	4574/0/321	4779/40/316	3837/40/316	1695/0/101
GOF F^2	1.091	1.127	1.109	1.030	1.024	1.021	1.018	1.076
R_1, wR_2 [$I>4\sigma(I)$]	0.0287, 0.0715	0.0433, 0.1096	0.0319, 0.0824	0.0303, 0.0787	0.0247, 0.0555	0.0372, 0.0529	0.0379, 0.0951	0.1011, 0.2477
R_1, wR_2 (all data)	0.0298, 0.0723	0.0463, 0.1188	0.0341, 0.0836	0.0418, 0.0829	0.0314, 0.0577	0.0865, 0.0952	0.0559, 0.1024	0.1247, 0.2668
largest diff. peak/hole [e Å^{3-}]	1.27, −1.76	2.11, −2.87	1.29, −1.04	0.9, −1.21	1.20, −1.01	1.34, −1,46	1.38, −1,62	3.49, −2.61

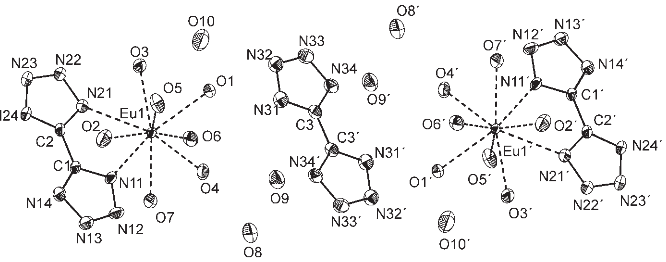

Figure 4. Motif of **5** (thermal ellipsoids represent 50 % probability), hydrogen atoms are omitted for clarity; selected bond lengths [Å] and angles [°]: Eu1–O1 2.394(15), Eu1–O2 2.526(15), Eu1–O3 2.451(8), Eu1–O4 2.384(12), Eu1–O5 2.480(9), Eu1–O6 2.46(2), Eu1–O7 2.433(11), Eu1–N11 2.698(6), Eu1–N21 2.59(2); O5-Eu1-O6 126.02(7), O4-Eu1-N21 135.13(14), O5-Eu1-O2 138.94(12), O1-Eu1-N21 120.25(13), O6-Eu1-O2 76.44(13), O7-Eu1-N21 114.05(12), O5-Eu1-O4 77.77(14) O3-Eu1-N21 69.54(12), O6-Eu1-O4 83.91(13), N11-Eu1-N21 62.95(13), O2-Eu1-O4 138.78(15), O5-Eu1-O1 67.81(11), O6-Eu1-O1 70.02(12), O2-Eu1-O1 130.37(12), O4-Eu1-O1 72.63(13), O5-Eu1-O7 135.52(11), O6-Eu1-O7 68.61(12), O2-Eu1-O7 69.65(11), O4-Eu1-O7 69.50(14), O1-Eu1-O7 125.71(11), O5-Eu1-O3 87.95(12), O6-Eu1-O3 82.42(12), O2-Eu1-O3 72.14(13), O4-Eu1-O3 140.77(13), O1-Eu1-O3 68.14(11), O7-Eu1-O3 136.20(11), O5-Eu1-N11 76.10(13), O6-Eu1-N11 137.62(13), O2-Eu1-N11 91.16(13), O4-Eu1-N11 79.42(14), O1-Eu1-N11 137.95(12), O7-Eu1-N11 69.08(11), O3-Eu1-N11 132.48(12), O5-Eu1-N21 70.50(12), O6-Eu1-N21 140.53(14), O2-Eu1-N21 68.97(15); symmetry operation for equivalent atoms: i: 3−*x*, 1−*y*, 1−*z*.

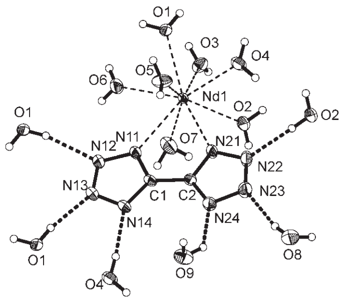

Figure 5. Description of N···H_2O contacts in **3** (thermal ellipsoids represent 50 % probability). Selected bond lengths [Å] and angles [°]: H042–N12 2.06(5), H043–N13 1.98(8), H9–N14 2.02(7), H031–N24 1.96(8), H032–N23 2.00(6), H2–N22 1.91(9); O1-H16-N12 172(5), O1-H24-N13 170(7), O4-H9-N14 173(7), O9-H22-N24 165(8), O8-H13-N23 154(7), O2-H2-N22 172(8).

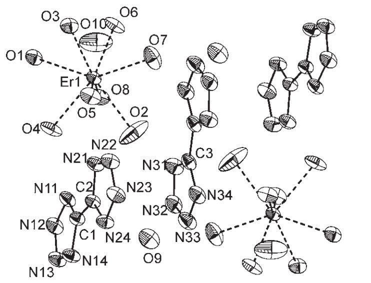

Figure 6. Motif of **7** (thermal ellipsoids represent 50 % probability), hydrogen atoms are omitted for clarity. Selected bond lengths [Å]: Er1–O1 2.41(2), Er1–O2 2.35(3), Er1–O3 2.35(4), Er1–O4 2.32(2), Er1–O5 2.332(14), Er1–O6 2.36(2), Er1–O7 2.328(18), Er1–O8 2.305(16); symmetry operator for equivalent atoms: i: −*x*, −1−*y*, 1−*z*.

tures of 5,5′-azotetrazolates,[5,16] bistetrazolatohydrazines,[19] and bistetrazolylamines.[18] The structures of **1** and **2** enable us to compare the chelate and bridging BT ligands. The C–C bond lengths of the bridging 5,5′-bitetrazoles are 1.456(8) Å for **1** (Figure 3) and 1.463(15) Å for **2**, nearly identical and in good agreement with characteristic C–C single bonds. The C–C bond lengths of the chelate type BT is 1.444(10) Å for (**1**) and 1.53(2) Å for (**2**). The C–N and N–N bond lengths in the aromatic tetrazole ring systems correspond to a bond order of 1.5 and also do not reveal any difference between chelate and bridging BT ligands.

The rare earth metal ions in **1** and **2** (Figure 3) are ninefold coordinated by six oxygen atoms from water molecules and by three nitrogen atoms N11 and N21 from a chelating ligand and N32 from the bridging ligand, forming a distorted tricapped trigonal prism. The bridging BT^{2-} is bonded through the nitrogen atoms at the 2- (N32) and 2′-positions (N32′) and the chelate BT^{2-} through the nitrogen atoms at the 1- (N11) and 1′-positions, (N21) (Figure 3). The distances between the rare earth metal ions and the coordinated oxygen atoms vary between 2.484(15) and 2.623(17) Å for **1** and between 2.45(3) and 2.72(3) Å for compound **2**, respectively. M–N distances vary between 2.61(2) and 2.80(3) Å for **1** and **2**. The molecular structures of **1** and **2** are best described as $[(\mu\text{-BT})\{M(BT)(H_2O)_6\}_2]\cdot 2\,H_2O$.

In complexes **3** to **5** (Figure 4), the metal atoms are coordinated by only one chelating BT^{2-} via the nitrogen atoms of the tetrazole ring at the 1- (N21) and 1′-positions (N11). Additionally, seven water molecules coordinate, forming a distorted tricapped trigonal prism, which represents a typical ninefold coordination for these metal centres. The rare earth metal–oxygen distances ranging from 2.384(2) to 2.51(6) Å are in good agreement with reported values of eight- and ninefold coordinated rare earth metal ions.[24–29]

The nitrogen atoms of the 5,5′-bitetrazolate ions in all complexes show evidence for weak bridges to water molecules. In **3** (Figure 5), N···O contacts of 2.774(13) and 2.89(2) Å can be interpreted in terms of N···H–O bridges, as the protons were found during the refinement process.[5] However, from their N···H distances and N···H–O angles they can be classified as only medium strong.[30]

The structures of **6** and **7** (Figure 6) can be classified as salt-like, comparable with the reported structures of 5,5′-azotetrazolate.[5,16] The rare-earth ions in complexes **6** and **7** are coordinated by eight water molecules forming a distorted square antiprismatic coordination. The shortest distances between the rare-earth metal and nitrogen are 4.37(3) Å for **6** and 4.35(4) Å for **7**. The rare earth metal–oxygen distances range between 2.337(12) and 2.437(17) Å for **6** and between 2.305(16) and 2.41(2) Å for **7**, noticeably shorter than in all other BT complexes, emphasising the salt-like nature of these derivatives.

An indication of the structure of 9: A remarkable bonding situation is observed in $[Sm(BTT)]\cdot 8\,H_2O$. Here, samarium builds up a molecular unit with BTT^{3-} acting as a tridentate ligand with three covalent Sm–N bonds.

Table 2. Bond lengths [Å^3] and angles [°] in BT complexes **1**–**7**.[a]

	1	**2**	**3**	**4**	**5**	**6**	**7**
C1−N11	1.337(6)	1.285(13)	1.333(6)	1.337(10)	1.338(13)	1.340(16)	1.332(11)
N11−N12	1.335(10)	1.43(2)	1.346(9)	1.345(18)	1.344(8)	1.34(2)	1.341(14)
N12−N13	1.306(7)	1.30 (15)	1.310(9)	1.308(18)	1.319(7)	1.308(13)	1.309(8)
N13−N14	1.351(6)	1.358(11)	1.347(8)	1.358(15)	1.346(10)	1.349(14)	1.341(10)
C1−N14	1.339(9)	1.395(17)	1.334(12)	1.32(2)	1.338(6)	1.336(17)	1.332(12)
C2−C1	1.444(10)	1.53(2)	1.456(9)	1.458(17)	1.453(9)	1.465(17)	1.460(12)
C2−N21	1.339(9)	1.379(16)	1.340(12)	1.33(2)	1.349(5)	1.327(17)	1.330(12)
N21−N22	1.342(7)	1.382(13)	1.347(8)	1.344(15)	1.344(9)	1.342(13)	1.343(10)
N22−N23	1.306(8)	1.280(16)	1.316(7)	1.314(15)	1.309(9)	1.301(12)	1.302(8)
N23−N24	1.343(11)	1.44(2)	1.342(10)	1.34(2)	1.355(8)	1.35(2)	1.338(14)
C2−N24	1.333(5)	1.297(10)	1.334(6)	1.322(11)	1.324(13)	1.338(15)	1.333(11)
C3−C3′	1.456(8)	1.463(15)	1.461(9)	1.474(17)	1.459(9)	1.47(2)	1.457(16)
C3−N31	1.333(6)	1.298(13)	1.339(6)	1.326(10)	1.337(13)	1.339(15)	1.339(11)
N31−N32	1.339(8)	1.386(15)	1.342(10)	1.342(18)	1.351(8)	1.328(17)	1.329(12)
N32−N33	1.320(8)	1.342(15)	1.312(8)	1.307(17)	1.311(9)	1.318(17)	1.313(12)
N33−N34	1.343(7)	1.305(13)	1.349(8)	1.349(15)	1.341(9)	1.34(2)	1.340(14)
C3−N34	1.337(10)	1.409(18)	1.338(12)	1.32(2)	1.339(6)	1.324(14)	1.330(10)
M−N11	2.726(17)	2.80(3)	2.64(2)	2.61(5)	2.698(6)		
M−N21	2.769(10)	2.66(2)	2.717(6)	2.695(12)	2.59(2)		
M−N32	2.741(11)	2.61(2)					
N11-M-N21	60.8(1)	61.2(1)	62.2(1)	62.7(2)	62.9(1)		
N24-C2-N21	111.9(2)	112.4(4)	112.0(4)	112.6(5)	112.2(4)	111.5(5)	112.4(6)
N24-C2-C1	128.3(2)	128.0(4)	128.5(4)	128.6(5)	128.6(4)	123.8(6)	123.2(7)
N21-C2-C1	119.8(2)	119.5(4)	119.4(4)	118.6(5)	119.1(4)	124.5(6)	124.2(7)
C2-N21-N22	104.5(2)	104.3(4)	104.4(4)	104.4(4)	104.3(4)	104.4(5)	104.1(6)
N23-N22-N21	109.4(2)	109.2(4)	109.6(4)	108.3(5)	108.8(5)	110.0(5)	110.5(7)
N22-N23-N24	110.1(2)	110.0(4)	109.4(5)	110.7(5)	110.4(4)	109.2(5)	109.1(6)
C2-N24-N23	104.1(2)	103.8(4)	104.4(4)	103.8(4)	104.2(4)	104.7(6)	103.7(6)
N11-C1-N14	111.5(2)	112.2(4)	112.6(4)	111.9(5)	112.1(4)	112.0(5)	111.2(7)
N11-C1-C2	120.3(2)	119.1(4)	119.2(4)	119.5(5)	118.6(4)	124.4(6)	124.7(7)
N14-C1-C2	128.2(2)	128.5(4)	128.1(4)	128.5(5)	129.2(4)	123.4(6)	124.0(7)
C1-N11-N12	105.2(2)	104.4(4)	104.4(4)	104.7(5)	103.8(4)	104.5(6)	104.4(7)
N13-N12-N11	109.4(2)	109.1(4)	108.3(4)	109.3(4)	109.8(4)	109.3(5)	109.9(6)
N12-N13-N14	110.1(2)	110.0(4)	110.4(4)	109.4(5)	109.5(5)	109.8(5)	109.3(7)
C1-N14-N13	103.9(2)	104.1(4)	104.1(4)	104.6(4)	104.7(4)	104.2(5)	104.9(7)
N34-C3-N31	111.6(2)	111.9(5)	111.4(4)	112.1(5)	111.3(5)	110.5(6)	111.8(7)
N34-C3-C3′	124.2(3)	124.1(4)	125.0(4)	125.1(5)	125.4(5)	124.7(6)	125.3(7)
N31-C3-C3′	124.2(2)	123.8(4)	123.5(4)	122.6(5)	123.1(5)	124.6(7)	122.7(7)
C3-N31-N32	104.4(2)	103.8(4)	105.1(4)	104.9(5)	105.4(4)	105.2(6)	104.3(7)
N33-N32-N31	110.3(3)	110.4(4)	109.5(4)	108.9(4)	108.7(4)	109.3(6)	109.4(7)
N32-N33-N34	108.4(2)	108.9(4)	109.4(5)	110.0(5)	109.9(5)	109.3(7)	109.6(8)
C3-N34-N33	105.2(3)	104.7(4)	104.4(4)	103.9(5)	104.5(4)	105.4(6)	104.6(7)

Unfortunately, the quality of the crystal structure is not very high (see Table 1). One reason for this might be that the structure was solved in the triclinic crystal system and the final symmetry (*C*2/*c*) was achieved by using ADDSYM in PLATON.[31] It might also be due to poor crystal quality. However, the bonding parameters within the ligand show a very high degree of similarity to the complex $[Ni(BMTT)_2]$ (BMTT = 1,3-bis(2-methyltetrazol-5-yl)triazenide).[21] Therefore, we consider a detailed discussion of the structure to be justified, particularly as the observed bonding mode of Sm to the triazenide is rather unusual. Typically, triazenide ligands bind in a chelate fashion via the N1 and N3 (in our case numbered N1 and N1′) atoms to rare earth metal ions.[32]

As depicted in Figure 7, Sm^{III} is coordinated by three nitrogen atoms N11, N2 and N11′ of the BTT^{3-} ligand and six oxygen atoms from water molecules, forming a distorted tricapped trigonal prism. At the same time, the two tetrazole rings and the trinitrogen bridge of BTT form a symmetrical plane including the Sm−N11, Sm−N2 and Sm−N11′ bonds. This fact, together with the bonding parameters for the tetrazole ring N1−N2 1.31(2), N1−C1 1.39(2), N11−N12 1.35(2), N12−N13 1.32(2) and N13−N14 1.37(2) Å, suggests an elongated π-system. The Sm−O distances for the water ligands are 2.389(16) (Sm−O3), 2.47(3) (Sm−O2) and 2.51(2) Å (Sm−O1) and comparable with those found for the Sm−BT complex **4**. However, the bond lengths for Sm−N11 or Sm−N11′, respectively, are significantly shorter (2.53(2) Å) than those of **4** and all other BT complexes described in this paper. The Sm−N2 distance lies at 2.737(16) Å, which is only slightly longer than M-N(tetrazolato) distances in **1** to **5**. Therefore, we consider it to be a bonding interaction.

Finally, we measured the IR spectrum of a KBr pellet of $[Sm(BTT)]\cdot 8H_2O$ (**9**) (Figure 8) and performed DFT calculations of the molecular vibrations using C_1 symmetry.

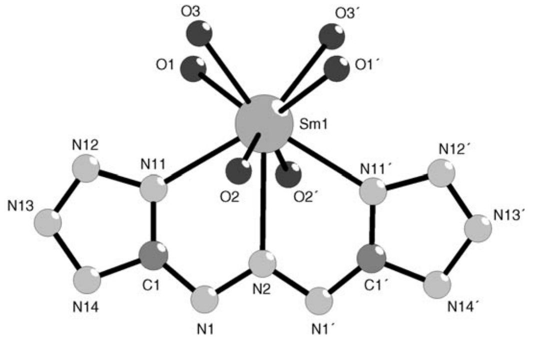

Figure 7. View on the coordinating unit of **9**.

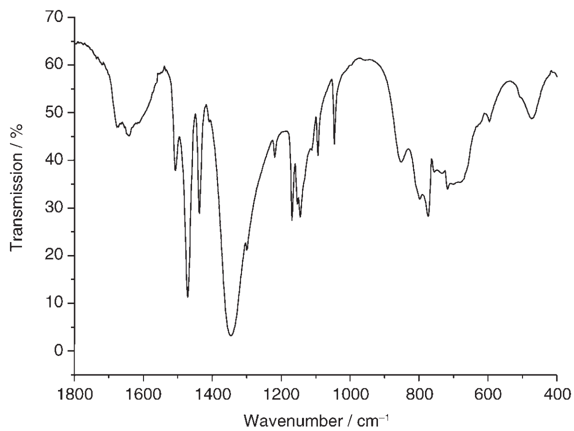

Figure 8. IR spectrum of [Sm(BTT)]·8 H_2O (**9**).

Table 3 lists the values obtained and reveals a high degree of congruency between measured and calculated values. In particular, the ν_{as}(N-N-N)$_{triaz}$ vibration at $\tilde{\nu} = 1346$ cm^{-1} seems to be characteristic for the BTT ligand.

Table 3. Calculated and observed IR frequencies for [Sm(BTT)]·8 H_2O (**9**).

Calculated B3LYP		Observed	
$\tilde{\nu}$ [cm^{-1}]	Intensities [%]	$\tilde{\nu}$ [cm^{-1}]	Assignment[a]
496.88	0.02	473.74	
628.11	0.12	595.75	
673.91	0		
675.05	0.02		
718.53	0		
723.81	1.42	717.47	
739.41	0.73	773.82	
887.67	2.41	798	
935.21	3.19	851.95	
942.29	0.35		
953.65	0.87		
983.70	0.03		
1054.43	5.09	1045.60	ν(N-N)$_{ring}$
1055.77	4.19		
1099.16	0.21	1093.14	ν(C-N-N)$_{ring}$
1120.27	1.21	1144.93	ν(N-N)$_{ring}$
		1152.99	ν(N-N)$_{ring}$
		1168.15	ν(N-N)$_{ring}$
1227.56	3.01	1218.73	
1228.93	0.81		
1257.44	1.5		
1281.15	2.3	1299.39	
1342.78	10.73		
1349.37	100	1346.05	ν_{as}(N-N-N)$_{triaz}$
		1437.47	
1479.01	20.92	1471.07	
1483.01	0.44	1507.08	
		1642.09	ν(C$_{ring}$-N$_{triaz}$)$_{ip}$
		1675.54	ν(C$_{ring}$-N$_{triaz}$)$_{oop}$

[a] ip = in plane; oop = out of plane.

Conclusion

5,5′-Bitetrazolate (BT^{2-}) and 1,3-bis(1*H*-tetrazol-5-yl)-triazenate (BTT^{3-}) are suitable ligands for the synthesis of multinuclear metal complexes and networks. Compounds such as **1** to **11** are prepared in water from conveniently accessible starting materials. The BT complexes obtained all exhibit the composition [$M_2(BT)_3$]·x H_2O with varying water content. The molecular structures of the BT complexes reveal three different complex structural types with a decreasing tendency to coordinate the BT^{2-} ligand as the rare earth metal ions are varied from La to Er. This tendency is in full agreement with the decreasing ionic radii along this series (Figure 9) and the increasing Lewis acidic character (manifested in the increasing hydration enthalpy), allowing coordination compounds for the early M elements, but favouring salt-like compounds for the heavier analogues.

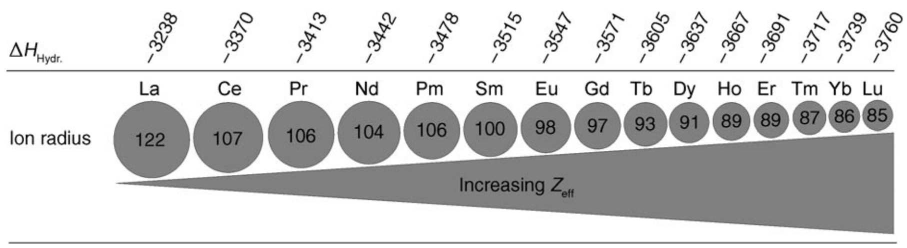

Figure 9. Relationship between increasing Z_{eff}, ion radius [pm] and hydration enthalpy [kJ mol^{-1}] of the trivalent rare earth metal ions.

Thus, the appropriate choice of rare earth metal ions and BT^{2-} ligands has enabled us to walk along the borderline between coordination and the formation of salt-like compounds. Unfortunately, the preliminary results presented here are limited to the crystal and molecular structures in the solid state and thus, we cannot make a statement on the coordination behaviour in solution.

Experimental Section

General remarks: Due to the explosive nature of most of the materials, safety equipment, such as leather gloves, a face-shield and ear protection are strongly recommended. Therefore, only a few KBr pellets (IR spectroscopy) were prepared and no Raman measurements were performed because the laser beam may ignite the compounds. All NMR spectra were recorded from concentrated (approximately 6 M) solutions in D_2O at ambient temperature on a Bruker Avance 400 MHz spectrometer; data are given in ppm. Elemental analyses were performed by using a HEKAtech Euro EA 3000 analyser. The differential temperature analysis measurement was performed with a Netzsch STA 409 DSC/TG unit. About 10 mg of **5** was used for the experiment. High resolution negative ESIMS spectra were measured on a Finnigan 900S spectrometer equipped with a double focusing sector analyser and a quadrupole ion trap at flow rates of approximately 1–5 $\mu L\,min^{-1}$ (1×10^{-5} $mol\,\mu L^{-1}$ in H_2O/MeOH). IR spectra were recorded with a Nicolet 5PC FTIR spectrophotometer by using KBr pellets. The powder diffraction pattern was collected by using a Huber G670 diffractometer operating with $Mo_{K\alpha}$ radiation ($\lambda = 0.71073$ Å; see Supporting Information). DFT calculations were carried out by using the program package TURBOMOLE 5.7.[33] The structure and frequency calculations were performed with the hybrid functional B3LYP[34] by using Ahlrichs triple-ζ valence plus polarisation (TZVP) basis set.[35]

X-ray crystallographic studies: Single crystals of **1–7** were obtained from aqueous solutions by slow evaporation in air. Suitable crystals were fixed in glass capillaries and transferred onto the diffractometer. Compounds **1–7** were measured on a STOE IPDS diffractometer by using graphite monochromated $Mo_{K\alpha}$ radiation ($\lambda = 0.71073$ Å). All calculations were performed by using SIR92[36] and SHELXL-97.[37] All non-hydrogen atoms were refined anisotropically. Hydrogen atoms could be located in the Fourier map and were refined isotropically. The numerical absorption corrections (X-RED V1.22; Stoe & Cie, 2001) were performed after optimising the crystal shapes by using X-SHAPE V1.06 (Stoe & Cie, 1999).[38]

Crystals of [Nd(BTT)] (**8**) and [Sm(BTT)] (**9**) were obtained in the same way. The cell constants $a=9.07$, $b=9.31$ and $c=11.04$ Å; $\alpha=99.52$, $\beta=93.35$ and $\gamma=112.54°$ for **8** and $a=9.10$, $b=9.45$ and $c=10.93$ Å; $\alpha=99.23$, $\beta=93.10$ and $\gamma=112.98$ for **9**, determined after 6000 reflections, are comparable. Unfortunately, only **9** could be solved by direct methods[36] in the triclinic crystal system. Additional symmetry (final space group: *C*2/*c*) was added by ADDSYM in PLATON.[31] Relevant data concerning crystallographic data collection and refinement are compiled in Table 2. CCDC 660545 (**1**), 660546 (**2**), 660547 (**3**), 660548 (**4**), 660549 (**5**), 660550 (**6**), 660551 (**7**) and 660713 (**9**) contain the supplementary crystallographic data for this paper. These data can be obtained free of charge from The Cambridge Crystallographic Data Centre via www.ccdc.cam.ac.uk/data_request/cif.

Barium 5,5′-bitetrazolate: Manganese 5,5′-bitetrazolate (81 g, 0.42 mol) and barium sulphide (71.84 g, 0.42 mol) were suspended in water and stirred under anaerobic conditions. After three days of stirring, the suspension was filtered and the solid extracted with water. The water phases were combined and the water distilled off to yield a colourless solid which was dried in vacuo at 100 °C (80 g, 70 %). ^{13}C NMR (100 MHz, D_2O, TMS): $\delta = 154.3$ ppm (s); MS (negative ESI): *m*/*z* (%): 137.17 (100) [$C_2HN_8^-$]; elemental analysis calcd (%) for BaC_2N_8 (273.40): C 8.78, H 0.00, N 40.98; found: C 8.52, H 1.84, N 39.64.

Sodium 5,5′-bitetrazolate: Manganese 5,5′-bitetrazolate (40 g, 0.21 mol) and sodium carbonate (22.2 g, 0.21 mol) were suspended in water (500 mL) and heated at reflux for several hours. Manganese carbonate was filtered off and the water evaporated to obtain a slightly green solid. After several recrystallisations from water, the solid became colourless and was dried in vacuo at 100 °C (25.2 g, 66 %). ^{13}C NMR (100 MHz, D_2O, TMS): $\delta = 154.3$ (s); MS (negative ESI): m/z (%): 137.17 (100) [$C_2HN_8^-$], 159.14 (10) [$NaC_2N_8^-$]; IR (KBr): $\tilde{\nu} = 1631$, 1458, 1345, 1327, 1307, 1182, 1148, 1072, 1048, 1016, 734, 586 (br) cm^{-1}; elemental analysis calcd (%) for $Na_2C_2N_8$ (182.05): C 13.19, H 0.00, N 61.55; found: C 12.94, H 0.0, N 59.21.

5,5′-Bitetrazole: Sodium 5,5′-bitetrazolate (20 g, 0.11 mol) was dissolved in water (150 mL) and aqueous hydrochloric acid was added dropwise until a colourless solid separated. The solid was filtered off, washed several times with cold water and dried in vacuo at 80 °C (3.8 g, 25 %); elemental analysis calcd (%) for $H_2C_2N_8$ (138.10): C 17.38, H 1.46, N 81.15; found: C 17.23, H 1.37, N 80.90.

Rare-earth 5,5′-bitetrazolate hydrates 1–7: In each case, barium 5,5′-bitetrazolate (1.15 g, 4.2 mmol) was dissolved in hot water (30 mL) and a solution of approximately 1 g (1.38 mmol) of the corresponding rare earth metal(III) sulphate hydrate in water (10 mL) was added. The precipitated barium sulphate was filtered off and the water evaporated to obtain a solid which was dried in vacuo at ambient temperature. Information about yields and elemental analyses of **1–7** are collected in Table 4.

*Complex **2***: IR (KBr): $\tilde{\nu} = 1691$, 1645, 1616, 1600, 1349, 1330, 1323, 1294, 1209, 1179, 1157, 1049, 1039, 1021, 668 cm^{-1} (br).

*Complex **6***: IR (KBr): $\tilde{\nu} = 1655$ (br), 1336 (vs), 1316, 1192, 1166, 1055, 1030, 756 cm^{-1} (br).

Na_2BT: IR (KBr): $\tilde{\nu} = 1631$, 1458, 1345, 1327, 1307, 1182, 1148, 1072, 1048, 1016, 734, 586 cm^{-1} (br).

Trisodium bis-tetrazolyltriazenate: This compound was synthesised according to the literature procedure.[22] Aminoguanidine nitrate (10 g, 72.9 mmol), sodium acetate (5 g, 60.9 mmol) and acetic acid (7.34 g, 122.2 mmol) were suspended in ice-cold water (50 mL) and a solution of sodium nitrite (7 g, 101.4 mmol) in water (30 mL) was added dropwise. After 12 h, the precipitated solid was collected and dissolved in water (50 mL) together with sodium hydroxide (1.45 g, 36.45 mmol). The water was evaporated in vacuo at ambient temperature to yield a light yellow solid that was recrystallised from ethanol and dried in vacuo at ambient temperature (5.36 g, 60 %). ^{13}C NMR (100 MHz, D_2O, TMS): $\delta = 171.4$ ppm (s); ^{15}N NMR (40 MHz, D_2O, $MeNO_2$): $\delta = 108.5$ (s, 1 N), −6.9 (s, 4 N), −93.7 (s, 2 N), −95.1 ppm (s, 4 N); MS (negative ESI): *m*/*z* (%): 180.15 (44) [$C_2H_2N_{11}^-$], 202.15 (100) [$NaC_2HN_{11}^-$]; elemental analysis calcd (%) for $Na_3C_2N_{11}\cdot 2H_2O$ (283.1): C 8.48, H 1.42, N 54.42; found: C 9.8, H 1.5, N 56.2.

Neodymium bis-tetrazolyltriazenate hydrate (8): Trisodium bis-tetrazolyltriazenate (0.28 g, 1 mmol) was dissolved in water (10 mL) and a solution of neodymium(III) chloride hydrate (0.82 g, 1 mmol) in water (10 mL) was added dropwise. After 12 h, gold metallic gleaming crystals that show a brown–colourless dichroism were obtained. Elemental analysis calcd (%) for $NdC_2N_{11}\cdot 8H_2O$ (466.5): C 5.15, H 3.46, N 33.03; found: C 5.36, H 2.83, N 33.63.

Samarium bis-tetrazolyltriazenate hydrate (9): Trisodium bis-tetrazolyltriazenate (0.28 g, 1 mmol) was dissolved in water (10 mL) and a solution of samarium(III) sulphate hydrate (0.37 g, 0.5 mmol) in water (10 mL) was added dropwise. After 12 h, gleaming metallic crystals that show a yellow–colourless dichroism were obtained. Elemental analysis calcd (%) for $SmC_2N_{11}\cdot 10H_2O$ (508.6): C 4.72, H 3.96, N 30.29; found: C 4.56, H 2.44, N 29.33.

Europium bis-tetrazolyltriazenate hydrate (10): Trisodium bis-tetrazolyltriazenate (0.28 g, 1 mmol) was dissolved in water (10 mL) and a solution of europium(III) sulfate hydrate (0.37 g, 0.5 mmol) in water (10 mL) was

Table 4. Yield and approximate composition of **1–7**.

Compound	1	2	3	4	5	6	7
colour	colourless	colourless	blue	yellow	colourless	colourless	pink
yield [g] ([%])	1.18 (81)	1.05 (71)	0.95 (64)	1.10 (73)	1.10 (73)	0.87 (57)	0.97 (63)
C [%] (calcd)[a]	6.60 (6.88)	6.77 (6.87)	6.78 (6.82)	6.63 (6.74)	6.70 (6.72)	6.49 (6.63)	6.64 (6.53)
H [%] (calcd)[a]	3.40 (3.85)	3.59 (3.84)	3.20 (3.81)	3.12 (3.77)	2.97 (3.76)	3.66 (3.71)	3.19 (3.65)
N [%] (calcd)[a]	30.70 (32.12)	31.80 (32.05)	31.08 (31.80)	31.40 (31.44)	31.7 (31.34)	30.4 (30.94)	30.9 (30.48)

[a] Calculated for a composition $[M_2(BT)_3]\cdot(H_2O)_{20}$.

added dropwise. After 12 h, a dark-yellow precipitate was obtained. Elemental analysis calcd (%) for $EuC_2N_{11}{\cdot}10H_2O$ (510.2): C 4.71, H 3.95, N 30.20; found: C 4.86, H 2.64, N 31.00.

Erbium bis-tetrazolyltriazenate hydrate (11): Trisodium bis-tetrazolyltriazenate (0.28 g, 1 mmol) was dissolved in water (10 mL) and a solution of erbium(III) sulphate hydrate (0.37 g, 0.5 mmol) in water (10 mL) was added dropwise. After 12 h, a yellow precipitate was obtained. Elemental analysis calcd (%) for $NdC_2N_{11}{\cdot}8H_2O$ (489.5): C 4.91, H 3.29, N 31.48; found: C 6.18, H 3.03, N 39.8.

Acknowledgements

We thank Dr. M. Schäfer for recording the negative ESIMS spectra as well as Dr. I. Pantenburg, I. Müller and H. Schumacher for the X-ray measurements.

[1] a) H. Gao, C. Ye, C. M. Piekarski, J. M. Shreeve, *J. Phys. Chem. C* **2007**, *111*, 10718–10731; b) R. P. Singh, R. D. Verma, D. T. Meshri, J. M. Shreeve, *Angew. Chem.* **2006**, *118*, 3664–3682; *Angew. Chem. Int. Ed.* **2006**, *45*, 3584–3601, and references therein.

[2] C. Ye, H. Gao, J. A. Boatz, G. W. Drake, B. Twamley, J. M. Shreeve, *Angew. Chem.* **2006**, *118*, 7420–7423; *Angew. Chem. Int. Ed.* **2006**, *45*, 7262–7265.

[3] a) J. Sauer, G. R. Pabst, U. Holland, H.-S. Kim, S. Loebbecke, *Eur. J. Org. Chem.* **2001**, 697–706; b) S. Loebbecke, A. Pfeil, H. H. Krause, J. Sauer, U. Holland, *Propellants, Explosives, Pyrotechnica* **2000**, *24*, 168–175.

[4] A. Hammerl, M. A. Hiskey, G. Holl, T. M. Klapötke, K. Polborn, J. Stierstorfer, J. J. Weigand, *Chem. Mater.* **2005**, *17*, 3784–3793.

[5] A. Hammerl, G. Holl, T. M. Klapötke, P. Mayer, H. Nöth, H. Piotrowski, M. Warchhold, *Eur. J. Inorg. Chem.* **2002**, 834–845.

[6] W. H. Binder, R. Sachsenhöfer, *Macromol. Rapid Commun.* **2007**, *28*, 15–54, and references therein.

[7] Some examples are 1,2,4,5-tetrazines: a) B. Sarkar, S. Frantz, W. Kaim, C. Duboc, *Dalton Trans.* **2004**, 3727–3731; b) N. S. Oxtoby, A. J. Blake, N. R. Champness, C. Wilson, *Proc. Natl. Acad. Sci. USA*, **2002**, *99*, 4905–4910; c) W. Kaim, *Coord. Chem. Rev.* **2002**, 230, 127–139; 2,2′-azopyridine (abpy): d) B. Sarkar, S. Patra, J. Fiedler, R. B. Sunoj, D. Janardanan, S. M. Mobin, M. Niemeyer, G. K. Lahiri, W. Kaim, *Angew. Chem.* **2005**, *117*, 5800–5803; *Angew. Chem. Int. Ed.* **2005**, *44*, 5655–5658; e) W. Kaim *Coord. Chem. Rev.* **2001**, 463, 219–221; 2,2′-azopyrazine: f) L. Carlucci, G. Ciani, D. M. Proserpio, S. Rizzato, *New J. Chem.* **2003**, *27*, 438–489; 2,2′-azobis(5-chloropyrimidine): g) S. Frantz, H. Hartmann, N. Doslik, M. Wanner, W. Kaim, H.-J. Kümmerer, G. Denninger, A.-L. Barra, C. Duboc-Toia, J. Fiedler, I. Ciofini, C. Uraban, M. Kaupp, *J. Am. Chem. Soc.* **2002**; *124*, 10563–10571; h) N. Doslik, T. Sixt, W. Kaim, *Angew. Chem.* **1998**, *110*, 2521–2522; *Angew. Chem. Int. Ed.* **1998**, *37*, 2403–2404; and 5,5′-bitriazole: i) W. Beck, F. Götzfried, M. Riederer, *Z. Anorg. Allg. Chem.* **1976**, *423*, 97–192; for general aspects of tetrazole chemistry see: R. N. Butler, *Adv. Heterocycl. Chem.* **1977**, *21*, 323–435.

[8] B. J. Coe, *Acc. Chem. Res.* **2006**, *39*, 383–393.

[9] a) *Nanoelectronics and Information Technology*, 2nd. ed. (Ed.: R. Waser), Wiley-VCH, Berlin, **2005**; b) N. Weibel, S. Gunder, M. Mayor, *Org. Biomol. Chem.* **2007**, *5*, 2343–2353; c) G. Pace, V. Ferri, C. Grave, M. Elbing, C. von Hänisch, M. Zharnikov, M. Mayor, M. A. Rampi, P. Samori, *Proc. Natl. Acad. Sci. USA* **2007**, *104*, 9937–9942; d) R. L. McCreery, *Anal. Chem.* **2006**, *78*, 3490–3497.

[10] N. K. Devaraj, R. A. Decreau, W. Ebina, J. P. Collman, C. E. D. Chidsey, *J. Phys. Chem. A* **2006**, *110*, 15955–15962.

[11] a) E. Oliveri-Mandala, *Gazz. Chim. Ital.* **1914**, *43*, 465–475; b) E. Oliveri-Mandala, *Gazz. Chim. Ital.* **1920**, *50*, 256–261; c) W. Friedrich, D.B.P. (D.B.P.: Deutsches Bundes-Patent) 952811, **1956**; d) G. I. Koldobskii, V. A. Ostrovskii, B. V. Gidaspov, *Khim. Geterotsikl. Soedin.* **1980**, *7*, 867–879 [*Chem. Abstr.* **1980**, *93*, 237969].

[12] V. Yu. Zubarev, V. A. Ostrowskii, *Chem. Heterocycl. Compd.* **2000**, *36*, 759–774.

[13] a) P. J. Steel, *J. Chem. Crystallogr.* **1996**, *26*, 399–402; b) J. H. Nelson, N. E. Takach, R. A. Henry, D. W. Moore, W. M. Tolles, G. A. Gray, *Magn. Reson. Chem.* **1986**, *24*, 984–994.

[14] A. J. Downard, P. J. Steel, J. Steenwijk, *Aust. J. Chem.* **1995**, *48*, 1625–1642.

[15] a) H. P. H. Arp, A. Decken, J. Passmore, D. J. Wood, *Inorg. Chem.* **2000**, *39*, 1840–1848; b) W. Selig, *Microchim. Acta* **1979**, 53–59.

[16] M. A. Pierce-Butler, *Acta Crystallogr. B* **1982**, *38*, 2681–2683.

[17] For recent examples, see a) I. V. Mendenhall, R. D. Taylor, *US Pat. Appl. Publ.* 2005-225692 20050913, **2006** [*Chem. Abstr.* **2006**, *146*, 103348]; b) M. W. Barnes, I. V. Mendenhall, R. D. Taylor, *US Pat. Appl. Publ.* 2004-899452 20040726, **2006** [*Chem. Abstr.* **2006**, *144*, 131369]; c) I. V. Mendenhall, *US Pat. Appl. Publ.* 2003-356012 20030131, **2004** [*Chem. Abstr.* **2004**, *140*, 166279].

[18] M. Friedrich, J. C. Gálvez-Ruiz, T. M. Klapötke, P. Mayer, B. Weber, J. J. Weigand, *Inorg. Chem.* **2005**, *44*, 8044–8052.

[19] A. Hammerl, G. Holl, M. Kaiser, T. M. Klapötke, H. Piotrowski, *Z. Anorg. Allg. Chem.* **2003**, *629*, 2117–2121.

[20] a) S. K. Sinha, K. Shankaran, K. R. K. Rao, *Indian J. Chem.* **1966**, *4*, 247–248; b) M. H. Friedman, *Combust. Flame* **1966**, *10*, 112–119.

[21] A. S. Lyakhov, P. N. Gaponik, D. S. Pytleva, S. V. Voitekhovich, L. S. Ivashkevich, *Acta Crystallogr. Sect. A* **2004**, *60*, m421–m422.

[22] a) J. Thiele, *Justus Liebigs Ann. Chem.* **1892**, *270*, 1–63; b) K. A. Hofmann, H. Hock, *Ber. Dtsch. Chem. Ges.* **1910**, *43*, 1866–1871.

[23] J. E. Huheey, Inorganic Chemistry, 3rd ed, Harper and Row, New York, **1983**.

[24] M. S. Wickleder, *Chem. Rev.* **2002**, *102*, 2011–2087.

[25] a) M. G. B. Drew, M. J. Hudson, P. B. Iveson, C. Madic, M. L. Russell, *J. Chem. Soc. Dalton Trans.* **1999**, 2433–2440; b) M. G. B. Drew, M. J. Hudson, P. B. Iveson, C. Madic, M. L. Russell, *J. Chem. Soc. Dalton Trans.* **2000**, 2711–2720.

[26] C. O. P. Santos, E. E. Castellano, C. C. Machado, G. Vincentini, *Inorg. Chim. Acta* **1985**, *110*, 83–86.

[27] R. D. Rogers, *Inorg. Chim. Acta* **1988**, *147*, 307–314.

[28] R. Ahmad, I. Dix, M. J. Hardie, *Inorg. Chem.* **2003**, *42*, 2182–2184.

[29] A. Chatterjee, E. N. Maslen, K. J. Watson, *Acta Crystallogr. Sect. B* **1988**, *44*, 381–386.

[30] T. Steiner, *Angew. Chem.* **2002**, *114*, 50–80; *Angew. Chem. Int. Ed.* **2002**, *41*, 48–76.

[31] A. L. Spek, PLATON (Version 150305), A Multipurpose Crystallographic Tool, University of Utrecht (Netherlands) or A. L. Spek, *J. Appl. Crystallogr.* **2003**, *36*, 7–13.

[32] a) H. S. Lee, M. Niemeyer, *Inorg. Chem.* **2006**, *45*, 6126–6128; b) S.-O. Hauber, M. Niemeyer, *Inorg. Chem.* **2005**, *44*, 8644–8646.

[33] R. Ahlrichs, M. Bär, M. Häser, H. Horn, C. Kölmel, *Chem. Phys. Lett.* **1989**, *162*, 165–169.

[34] a) A. D. Becke, *J. Chem. Phys.* **1993**, *98*, 5648–5652; b) P. J. Stephens, F. J. Devlin, C. F. Chabalowski, M. J. Frisch, *J. Phys. Chem.* **1994**, *98*, 11623–11627.

[35] A. Schäfer, C. Huber, R. Ahlrichs, *J. Chem. Phys.* **1994**, *100*, 5829–5835.

[36] SIR92—a program for automatic solution of crystal structures by direct methods, see A. Altomare, G. Cascarano, C. Giacovazzo, A. Guagliardi, M. C. Burla, G. Polidori, M. J. Camalli, *J. Appl. Crystallogr.* **1994**, *27*, 435–436.

[37] G. M. Sheldrick, SHELXL-97, a program for crystal structure refinement, University of Göttingen, Göttingen (Germany), **1997**.

[38] STOE X-RED, Data Reduction Program, Version 1.22/Windows, STOE & Cie, Darmstadt (Germany), **2001**; STOE X-SHAPE, Crystal Optimisation for Numerical Absorption Correction, Version 1.06/ Windows, STOE & Cie, Darmstadt (Germany), **1999**.

Received: December 19, 2007
Published online: March 3, 2008

